*Tellus (1995), 47B, 353–364*
*Printed in Belgium – all rights reserved*


TELLUS
*ISSN 0280–6509*

# Combined measurements of UV-A actinic flux, UV-A irradiance and global radiation in relation to photodissociation rates

By MICHIEL VAN WEELE[1]*, JORDI VILÀ-GUERAU DE ARELLANO[1] and FOEKE KUIK[2],
[1]*Institute for Marine and Atmospheric research Utrecht (IMAU), Utrecht University, Utrecht, The Netherlands*; [2]*Royal Netherlands Meteorological Institute (KNMI), De Bilt, The Netherlands*

(Manuscript received 29 April 1994; in final form 5 September 1994)

ABSTRACT

At present, photodissociation rates at ground level are mainly estimated from empirical expressions that relate the irradiance (UV-A or global) to photodissociation rates. In this paper, a comparison is made between the UV-A actinic flux, which is the appropriate radiometric quantity to estimate photodissociation rates, and the two other commonly used radiometric quantities: UV-A irradiance and global radiation. The comparison is based on measurements of the 3 quantities at various locations: the Azores (37° N), Antarctica (74° S) and the Netherlands (52° N). The observed variation in UV-A actinic flux, simultaneously measured UV-A irradiance and global radiation is a measure of the accuracy that can be obtained with empirical relations that relate UV-A irradiance or global radiation to photodissociation rates. It is shown that solar zenith angle, surface albedo and the ratio of direct downward to total downward irradiance are the main factors that determine the relation between UV-A actinic flux and UV-A irradiance at ground level. However, the angular distribution of the radiation field is also important. Model calculations using a doubling-adding code show large variations in the actinic flux for a given irradiance because of the anisotropy of the radiation field. When the atmosphere is cloud-free and unpolluted and also when the sky is completely overcast, UV-A actinic fluxes for a given UV-A irradiance are found to vary by about 10% at ground level. Therefore we also estimate that empirical relations between photodissociation rates and UV-A irradiance are accurate within 10% under these well-defined circumstances. Horizontal inhomogeneity of the atmosphere enlarges the uncertainty in the relation between actinic flux and irradiance. Variations of up to 25% in UV-A actinic flux for a given UV-A irradiance were observed on a day with partial cloud cover. Variations in UV-A actinic fluxes for a given global radiation measurement were always less than 20%, i.e., for clear sky, completely overcast conditions and partial cloud cover conditions.

## 1. Introduction

Important chemical species in the troposphere such as ozone ($O_3$), nitrogen dioxide ($NO_2$), formaldehyde ($CH_2O$) and hydrogen peroxide ($H_2O_2$) are photodissociated by sunlight. The most important spectral region where dissociation of these species takes place is the UV-A spectral region [315–400 nm], which is mainly outside the ozone absorption bands. In the troposphere ozone is dissociated in the UV-B spectral region only [290–315 nm].

In experimental campaigns carried out to study tropospheric chemistry accurate estimates of photodissociation rates are important for data analysis (MLOPEX: Shetter et al., 1992; CITE 3: Davis et al., 1993). Direct measurements of the photodissociation rate of $NO_2$ ($J_{NO_2}$) with a chemical actinometer can be performed within an

* Corresponding author.

accuracy of about 5% according to Shetter et al. (1992). However, this type of measurements is experimentally complicated. Therefore, to date empirical expressions are used that relate $J_{NO_2}$ to radiometer measurements and then photodissociation rates of other chemical species are assumed to relate to $J_{NO_2}$.

The empirical expressions for the photodissociation rate of $NO_2$ were derived from simultaneous measurements of $J_{NO_2}$ taken with a chemical actinometer and radiometric measurements of UV-A irradiance (Madronich, 1987a; Shetter et al., 1992) and global radiation (Bahe et al., 1980). Both radiometric quantities are measured with a flat sensor, i.e., the instrument responses depend on the direction of the incident radiation. However, photodissociation rates are not proportional to the radiation incident on a surface but are proportional to the actinic flux (Madronich, 1987b). The actinic flux is defined as the spherical integrated light intensity (radiance) directed to a certain point or molecule in space (in units of Watts per square meter per wavelength interval). Therefore, the actinic flux differs from the irradiance, i.e., the hemispheric integrated radiance incident on a flat surface.

We present actinic flux measurements made using a photo-electric detector (van der Hage et al., 1994). The only direct actinic-flux measurements reported previously were those made by Nader and White (1969), Van der Hage (1992) and Vilà-Guerau de Arellano et al. (1994). A photoelectric detector that measures specific photolysis rates was developed by Junkerman et al. (1989). Measurements of $J_{NO_2}$ using this instrument (i.e., indirect actinic flux measurements) were presented by Brauers and Hofzumahaus (1992).

In this paper we study the accuracy of the empirical expressions that relate $J_{NO_2}$ at ground level to UV-A irradiance and global radiation measurements. We present measurements of UV-A actinic flux, in combination with simultaneous measurements of UV-A irradiance and global radiation. Measurements were performed at various locations: the Azores (37°N), Antarctica (74°S) and the Netherlands (52°N). An extensive set of meteorological data is available for all sites.

Differences in the effects of surface albedo, (partial) cloudiness, latitude, season and aerosol content on UV-A actinic flux, UV-A irradiance and global radiation can be quantified using the combined data set. Madronich (1987a) explained that the photodissociation rate of $NO_2$ can be related to UV-A irradiances when surface albedo, solar zenith angle and the ratio of direct and total incident radiation are known. Here we show that these parameters are indeed the most important in the relation between UV-A irradiance and UV-A actinic flux under all atmospheric and surface conditions. However, we also show that it is not always possible to obtain accurate estimations of photodissociation rates (actinic fluxes) from irradiance measurements because of the anisotropy of the radiation field and the horizontal inhomogeneity of the atmosphere. Model calculations of Ruggaber et al. (1993) showed that even in the case of horizontally homogeneous atmospheres neglect of the full angular distribution of the radiation field can produce errors up to 20% in the photodissociation rates.

A comparison is made between the radiometric measurements and radiative transfer calculations. We use a $\delta$-Eddington code (Van Weele and Duynkerke, 1993) and also a doubling-adding code developed at KNMI (Stammes, 1993), based on algorithms from Van de Hulst (1980) and De Haan et al. (1987). The latter takes the full angular distribution of the radiation field into account and consequently the effect of anisotropy can be studied. Physical processes included in both models are Rayleigh scattering, ozone absorption, clouds and aerosol extinction. Boundary conditions are provided by the extraterrestrial solar flux, solar zenith angle and surface albedo.

Finally we show that global radiation can be used to estimate $J_{NO_2}$ instead of UV-A irradiance measurements with at most a small reduction in accuracy.

## 2. Instrumentation and sites

### 2.1. *Description of the instruments*

The UV-A actinic flux was measured using a photo-electric detector in the wavelength region between 330 and 390 nm. The detector is housed in a plastic cylinder from which six sensors protrude, arranged according to cubic symmetry. Details about the instrument's calibration and the directional response are given elsewhere (Van der Hage et al., 1994). It was shown theoretically and experimentally that the directional response of the

instrument is isotropic within 5%. The photo-electric detector has been successfully used to measure vertical profiles of actinic flux in the marine cloud-topped boundary layer (Vilà-Guerau de Arellano et al., 1994). The frequency of the measurements presented here is 0.1 Hz, although we usually show 10-min averages. Only in the case of partial cloudiness (Fig. 3) do we give 1-min averages.

The UV-A irradiance measurements were made using a narrow-band Kipp & Zonen (Delft, The Netherlands) CUVA1 irradiance meter with a central wavelength at 367 nm and a full-width half-maximum (FWHM) of 10 nm. The meter was calibrated with a 1000 W NIST calibrated lamp. The frequency of the measurements is 0.04 Hz. Data presented in this paper are 10-min averages.

The instrument response functions of the photo-electric detector and the irradiance meter are not exactly the same. So that measurements could be compared both spectral integrated signals were corrected for the difference in band width. As a result the UV-A actinic flux and UV-A irradiance presented in this paper are always given in units of $W\,m^{-2}\,nm^{-1}$. The resulting estimated precision of the UV-A actinic flux and UV-A irradiance measurements presented is typically better than 10%.

Global radiation observations were made with a Kipp & Zonen CM11 pyranometer that measures the solar irradiance for wavelengths between about 305 and 2800 nm with a precision of 2%. These measurements were also recorded with 0.04 Hz frequency and averaged over 10-min intervals.

### 2.2. *Description of the sites*

The first radiometric measurements (actinic flux and global radiation) were carried out within the framework of the Atlantic Stratocumulus Transition EXperiment (ASTEX) (ASTEX, 1992). The observations were made between 1 and 30 June 1992 on Santa Maria island (36.99° N; 25.17° W), the Azores. The local UV-A albedo of the surface site was measured by pointing 1 of the 6 sensors of the photo-electric detector downward and upward alternately while the other 5 were kept covered. In this UV spectral region the average albedo was found to be about 0.05. The site was located 50 m above sea level in a meadow covered with ochre-coloured dry grass.

Actinic flux and global radiation measurements were also performed above a blue-ice surface in the Heimefront Range (74.58° S; 11.22° W), Queen Maud Land, Antarctica between 30 December 1992 and 7 January 1993. The site is located approximately 1200 m above sea level. The UV-A surface albedo at the site was not measured. We assume that the value is about 0.9 (Warren et al., 1993). This value is also based on the albedo measured for the whole short-wave spectral region.

Continuous measurements of UV-A actinic flux, UV-A irradiance and global radiation were made in De Bilt (52.00° N; 5.18° W), the Netherlands between 18 June and 6 July 1993. De Bilt is located approximately at sea level. Measurements were performed on the roof of the Royal Netherlands Meteorological Institute (KNMI) about 15 m above street level with a 95% free horizon. The UV-A surface albedo at this site was also about 0.05.

The measurements at the different locations were all performed around the summer solstice. Therefore, the radiometric quantities were measured while the solar zenith angle was at its yearly minimum.

## 3. The relation between UV-A actinic flux and UV-A downward irradiance

The actinic flux $F$ is defined as the radiance integrated over all solid angles. The actinic flux can be decomposed into three terms: a diffuse downward flux $F_{\downarrow}$, a diffuse upward flux $F_{\uparrow}$ and a direct downward flux $F_0$. The downward irradiance $E$ is defined as the radiance weighted with the cosine of the angle of incidence integrated over the overlying hemisphere. The downward irradiance can be decomposed into two terms: a diffuse downward flux $E_{\downarrow}$ and a direct downward flux $E_0$. Irrespective of atmospheric conditions the ratio of actinic flux to the downward irradiance above a (Lambertian) reflecting surface with albedo $A$ can be expressed as:

$$\frac{F}{E} = 2(1+A) + \left(\frac{1}{\mu_0} - 2\right)\frac{E_0}{E}, \tag{1}$$

where $\mu_0$ is the cosine of the solar zenith angle. The Appendix shows how eq. (1) is derived. It is impor-

tant to mention that eq. (1) is only an approximation of the exact ratio given by eq. (A6) in the Appendix. In eq. (1), the angular distribution of the radiation field is prescribed. The accuracy of this assumption will be discussed later. First we discuss some basic features of eq. (1).

Both monochromatic fluxes and fluxes that are integrated over the same spectral interval satisfy eq. (1). Further, eq. (1) shows that the ratio of actinic flux to downward irradiance depends on surface albedo, the solar zenith angle and the ratio of direct to total downward irradiance. Below a thick cloud ($E_0 = 0$) a linear relationship is found between the actinic flux and the downward irradiance, the proportionality factor being determined by surface albedo. In all other cases a non-linear relation is found between $F$ and $E$. Similar non-linear behaviour in the relation between the photodissociation rate of $NO_2$ and UV-A irradiance was described by Harvey et al. (1977), Zafonte et al. (1977) and Madronich (1987a). This non-linear behaviour is most pronounced for small zenith angles. For $\mu_0 > 0.5$ the non-linear term is negative. When $\mu_0$ approaches zero, the non-linear term also approaches zero ($E_0 = \mu_0 F_0$).

Eq. (1) shows that the actinic flux and the downward irradiance do not have the same diurnal variation. Around noon, i.e., at small zenith angles and when there is a large contribution of the direct incident radiation, the second term in eq. (1) is large and is negative. Therefore, the actinic flux varies more slowly in time than does the irradiance. This flattening out of the diurnal variation, characteristic for the actinic flux (Van der Hage, 1992), will be most pronounced at low latitudes where the relative contribution of direct radiation will be largest around noon.

A formulation similar in concept to eq. (1) was derived by Madronich (1987a): see eq. (9) and Fig. 5 in his paper. However, the formulation used here is advantageous because the two unknown parameters ($A$ and the ratio $E_0/E$) can be measured directly. The ratio $E_0/E$ can also easily be parameterized. Therefore, there is no need to make multiple scattering calculations, such as were made by Madronich (1987a). In the following section we will give a parameterization for the ratio of $E_0/E$. Afterwards we discuss the effect of the angular distribution of the radiation field on the relation between $F$ and $E$.

### 3.1. *Parameterization of the ratio $E_0/E$*

In cases where the ratio of the direct incident irradiance to total incident irradiance ($E_0/E$) is not measured it is advantageous to use a parameterization. Following the Lambert-Beer law, we find for the direct downward component of the incident radiation at ground level $E_0 = \mu_0 S_0 \exp(-\tau_a/\mu_0)$, where $S_0$ is the solar flux at the top of the atmosphere perpendicular to the incident radiation, $\tau_a$ is the optical thickness of the total atmosphere and $\mu_0$ is the cosine of solar zenith angle.

In the UV-A spectral region, molecular scattering is important, whereas absorption (mainly by $NO_2$ and aerosols) is relatively small. Therefore we assume that radiation is removed from the incident beam (equal to $\mu_0 S_0 - E_0$) by scattering only. A fraction $\alpha$ of the scattered radiation will reach the surface. Then, the diffuse downward irradiance $E_\downarrow$ can be written as:

$$E_\downarrow = \alpha \mu_0 S_0 [1 - e^{-\tau_a/\mu_0}] \tag{2}$$

For isotropic (molecular) scattering, i.e., in a unpolluted, clear sky atmosphere $\alpha = 0.5$, i.e., half of the scattered radiation is scattered upward and half is scattered downward. When anisotropic (forward) scattering by clouds and aerosols are important, somewhat higher values for $\alpha$ occur (typically $\alpha < 0.7$).

Further, above highly reflecting surfaces (snow) multiple scattering between the Earth surface (with albedo $A$) and the atmosphere (with spherical albedo $\beta$) may be important. As a result the total incident irradiance $E$ is enhanced by a factor $1 + \beta A + \beta^2 A^2 + \cdots = (1 - \beta A)^{-1}$. Mostly the correction is small because the surface albedo $A$ is small for most surfaces in the UV-A region (see also Section 2). On the other hand, the atmosphere is optically rather thick in the UV-A region. Therefore the spherical albedo of the atmosphere is also relatively large. Model calculations show that in the UV-A region $\beta$ decreases almost linearly with wavelength from (typically) $\beta = 0.39$ (at $\lambda = 330$ nm) to $\beta = 0.25$ (at $\lambda = 390$ nm).

Combining $E = (1 - \beta A)^{-1} (E_0 + E_\downarrow)$ and eq. (2) yields

$$\frac{E_0}{E} = (1 - \beta A) \times \frac{e^{-\tau_a/\mu_0}}{e^{-\tau_a/\mu_0} + \alpha[1 - e^{-\tau_a/\mu_0}]} . \tag{3}$$

Eq. (3) can only be used when the optical thickness of the atmosphere $\tau_a$ is known. This parameter is strongly wavelength dependent. The optical thickness due only to molecular scattering (proportional with $\lambda^{-4}$) ranges from 0.4 at 390 nm to 0.8 at 330 nm. When clouds or aerosols are present larger values are found for $\tau_a$. The latter processes are typically broad-band effects, i.e., the wavelength dependence is small in the UV-A region. Furthermore, when $\tau_a$ is large, the ratio of $E_0/E$ approaches zero.

For all conditions where the term with $E_0/E$ in eq. (1) is important, i.e., for cloud free conditions and for zenith angles smaller than 60°, the accuracy of eq. (3) is better than 5% when the wavelength dependence of $\tau_a$ and $\beta$ is taken into account.

The combination of eqs. (1) and (3) shows how different atmospheric (clouds, aerosols) and geographic conditions (surface albedo, latitude) affect the ratio between the irradiance and the actinic flux. Actinic fluxes can be calculated from irradiances when solar zenith angle, surface albedo and the ratio of the direct downward to total downward irradiance are known. The last ratio can be parameterized in the UV-A region in cases where measurements are missing.

### *3.2. Angular distribution of the radiation field*

In the Appendix, it is shown that eq. (1) is valid for an isotropic radiation field as well as in the Eddington approximation (Shettle and Weinman, 1970). Unfortunately, the angular distribution of the radiation field is generally more complex than is described by the Eddington approximation. Extended radiative transfer calculations that take into account the full angular dependence of the radiation field are necessary in order to calculate actinic fluxes and irradiances more accurately (Ruggaber et al., 1993; Stammes, 1993). However, even the best available models still cannot handle effects of horizontal inhomogeneities such as clouds. Further, assumptions regarding the aerosol optical properties have to be made in model calculations. However, aerosol concentration and type in the atmosphere are highly variable.

The anisotropy of the radiation field can be estimated for horizontally homogeneous atmospheres. Under clear sky conditions the incident diffuse radiation is larger from the horizon than from the zenith. On the other hand, for overcast conditions the incident diffuse radiation is larger from the zenith than from the horizon. In the following we will discuss this so-called anisotropy of the radiation field. The effect was estimated quantatively using a radiative transfer code, taking into account the full angular distribution of the radiation field (De Haan et al., 1987; Stammes, 1993).

In a clear sky atmosphere, the incident diffuse radiation is larger from the horizon than from the zenith because for single, isotropic scattering the scattered radiation that is incident from a certain direction is determined by the number of scatterers along the line of sight. On the other hand, multiple scattering will tend to reduce the anisotropy because the optical thickness along the path of the scattered radiation is largest in the directions where most single scattered radiation originates. Thus, although most scattering occurs in the lowest layers of the atmosphere, the scattered radiation has to travel through a more dense atmosphere to reach the instrument.

The ratio of the diffuse downward actinic flux $F_\downarrow$ to the diffuse downward irradiance $E_\downarrow$ is equal to 2 for isotropic incident radiation (see Appendix). However, due to the directional dependence of the incident radiation we expect that in clear sky conditions $E_\downarrow$ will be smaller for the same $F_\downarrow$. For the 330–390 nm spectral region we performed radiative transfer calculations in order to determine the ratio $F_\downarrow/E_\downarrow$. We calculated $F_\downarrow/E_\downarrow = 2.25 \pm 0.25$ for a cloud free unpolluted atmosphere, depending on solar zenith angle and wavelength. The highest ratios are found for the longest wavelength (less multiple scattering). Anisotropic single scattering (e.g., by aerosols) can both enhance and diminish the angular distribution of the radiation field, depending on, for example, solar zenith angle. Therefore we believe that variations in the ratio $F_\downarrow/E_\downarrow$ under cloud free conditions are largely due to aerosols in the boundary layer.

For overcast conditions, the incident diffuse radiation is larger from the zenith than from the horizon. The reason is that in this situation multiple scattering in the cloud mainly determines the angular distribution of the radiation field below the cloud. Radiation inside the cloud will most probably leave the cloud in a direction perpendicular to cloud base. In all other directions the probability of another scattering event is larger.

Therefore below a cloud most scattered radiation incident at ground level originates from the zenith direction. Further, the optical thickness of the path through the atmosphere below the cloud is also smallest for the scattered radiation that is incident from the zenith. Therefore we expect that below a cloud $E_\downarrow$ is larger for the same $F_\downarrow$ compared to the case of isotropic incident radiation. Radiative transfer calculations for a surface albedo of 0.05 show typically $F_\downarrow/E_\downarrow = 1.70 \pm 0.05$ at ground level, almost independent of solar zenith angle, cloud optical properties and cloud height. For large surface albedo the ratio approaches its isotropic limit of 2.

Unfortunately, clouds are rarely horizontally homogeneous. Therefore the uncertainty in the ratio is larger than suggested by the model calculations. Furthermore, for thin clouds, i.e., with direct radiation below the cloud, or when aerosol scattering below the cloud is important, larger variations in the ratio of $F_\downarrow/E_\downarrow$ are found. In such cases the values depend strongly on wavelength, solar zenith angle, surface albedo and cloud optical properties and aerosol optical properties.

For all realistic horizontal homogeneous atmospheres (clear sky, small or large aerosol content, thin or thick clouds) model calculations show that typically $F_\downarrow/E_\downarrow = 2.0 \pm 0.5$ in the UV-A spectral region. Therefore we estimate that there will not be more than about 25% variation in the UV-A actinic flux for given UV-A irradiance because of the angular distribution of the radiation field, irrespective of atmospheric conditions. Horizontal inhomogeneities in the atmosphere can further contribute to this variation.

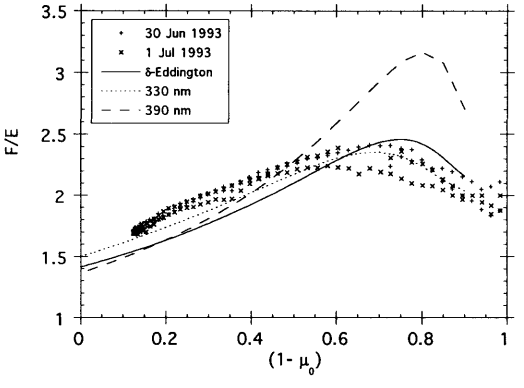


*Fig. 1.* The ratio of UV-A actinic flux ($F$) to UV-A irradiance ($E$) for clear sky conditions as a function of $(1-\mu_0)$. Measurements (30 June 1993 and 1 July 1993) are 10-min averages, performed in De Bilt, the Netherlands. The solid line was calculated with a $\delta$-Eddington model. Dashed lines were calculated with the doubling-adding model (for 330 nm and 390 nm).

The variation in UV-A actinic flux for given UV-A irradiance is drastically reduced when distinction is made between different atmospheric conditions. For unpolluted cloud free conditions when the relatively well-known direct radiation dominates the diffuse radiation, our model calculations suggest a variation of less than 10% in the ratio $F/E$ because of the angular distribution of the radiation field. Aerosol extinction leads to more variation. In overcast conditions the uncertainty is determined mainly by the horizontal inhomogeneities, which are difficult to assess with model calculations.

## 4. Observations of UV-A actinic flux and UV-A irradiance

We verified eq. (1) and the model calculations presented in the previous section by making simultaneous measurements of UV-A actinic flux and UV-A irradiance. Fig. 1 shows the ratio of $F/E$ for 2 days with clear sky conditions. In this figure we also included the ratio of the fluxes calculated with a $\delta$-Eddington model (Van Weele and Duynkerke, 1993). These calculations correspond to the use of eq. (1). However, we calculated the fluxes by integration over the 330–390 nm spectral region with 5 nm resolution and weighting them with the instrument response function. The calculated fluxes are expressed in units of $\mathrm{W\,m^{-2}\,nm^{-1}}$.

Both the measured and calculated ratios of $F/E$ are lowest for small zenith angle. This is due to the importance of the second term in eq. (1) which becomes negative for $\mu_0 > 0.5$. For larger zenith angle the $F/E$ ratio increases first before decreasing again when the sun reaches the horizon ($E_0 = 0$).

Some systematic differences are found between the measured and modelled ratios of $F/E$. These can be caused by systematic errors in (one of) the measured fluxes or by the assumptions in the model calculations. As explained in Van der Hage et al. (1993), the actinic flux is measured within an accuracy of 10%. However, the possibility that there is some systematic over- or underestimation

(but smaller than 10%) of measured actinic fluxes cannot be ruled out.

Uncertainties in the model calculations can also explain the observed differences, mainly because of the assumed aerosol characteristics (optical thickness 0.2, single scattering albedo 0.8, asymmetry parameter 0.85) and the use of the Eddington approximation for the angular distribution of the radiation field. Fluxes calculated with a $\delta$-Eddington model are typically accurate within 10% (Toon et al., 1990; King and Harsvardhan, 1986; Liou, 1992).

In order to assess the effect of the angular distribution of the radiation field we also performed some calculations with the doubling-adding code (Stammes, 1993). Monochromatic calculations for 330 nm and 390 nm were performed in order to show the maximum and minimum values for the ratio of $F/E$ in the UV-A spectral region. No aerosol scattering was included in these calculations. As expected from the discussion in Section 3 we see the largest deviations for the longest wavelengths (390 nm) at which single scattering is important. At 330 nm multiple scattering is important, and the radiation field becomes more isotropic. Therefore, the ratio of $F/E$ is less dependent on solar zenith angle at 330 nm than at 390 nm.

Fig. 2 shows the ratio of $F/E$ for 2 days with a completely overcast sky. No direct radiation at ground level was observed ($E_0 = 0$). The observed ratio of $F/E$ no longer depends on solar zenith angle, just as predicted by eq. (1). Measured values are mostly in the range 1.8 to 2.0. We calculated a mean value of $F/E = 1.91 \pm 0.14$ ($1\sigma$). Eq. (1) predicts a constant ratio $F/E = 2.1$ ($A = 0.05$). Model calculations that take into account the angular distribution of the radiation field yield $F/E = 1.83$ for all zenith angles and all wavelengths in the UV-A. When aerosol extinction below the cloud is included we find $F/E = 1.77$. We conclude that the observed ratios of $F/E$ correspond well with the values calculated with the model. The scatter in the data mainly reflects the horizontal inhomogeneity of the atmosphere which is difficult to include in any radiative transfer model.

It is seen that the variation in the ratio of $F/E$ is typically less than 10% for both clear sky conditions (Fig. 1) and for cases where no direct radiation at the ground is observed (Fig. 2). Under these conditions, therefore, empirical relations between photodissociation rates and UV-A irradiance measurements can be accurate within 10%.

In Fig. 3 actinic flux measurements are presented as a function of $1\text{-}\mu_0$ for a clear day and for a day with partial cloudiness. During the day with partial cloudiness a regular pattern of streets of cumulus clouds was advected over the measurement site. The data in the figure are 1-min averages. Occasionally we observe actinic fluxes that are 10% higher than the clear sky values. These increased values can be ascribed to extra scattering in the atmosphere as a result of the highly reflecting sides of clouds. The values for $F/E$

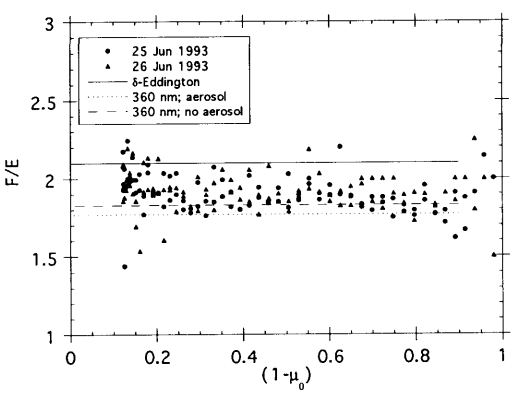


*Fig. 2.* The same as Fig. 1 but for overcast conditions at 25 June 1993 and 26 June 1993. The calculations with the doubling-adding model were performed for 360 nm.

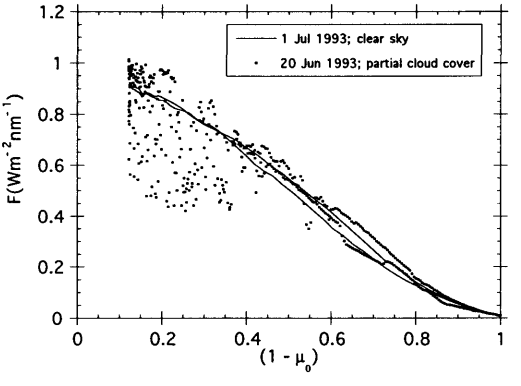


*Fig. 3.* Measurements of the 1-min averages of UV-A actinic flux as a function of $(1 - \mu_0)$ for a day with clear sky (1 July 1993) and a day with occasionally partial cloud cover conditions (20 June 1993) in De Bilt, the Netherlands.

for this day varied between the limits for clear sky and overcast conditions, i.e., $F/E = 2.0 \pm 0.5$. Therefore, for this situation emperical relations between photodissociation rates and UV-A irradiance can be accurate within 25%.

## 5. Observations of UV-A actinic flux and global radiation

It is advantageous to estimate photodissociation rates from global radiation (G) measurements that are made routinely at many meteorological stations. Therefore, Bahe et al. (1980) and Brauers and Hofzumahaus (1992) presented an empirical linear relation between G and the photodissociation rate of $NO_2$ ($J_{NO_2}$). In other words, they established a relation between the irradiance integrated over the short-wave solar spectrum and a quantity that is proportional with the UV-A actinic flux. However, assuming that the global radiation correlates well with the UV-A irradiance, we expect to find a distinct non-linear relation between global radiation and actinic flux. Furthermore, the linear part should depend on surface albedo.

First we compared our UV-A irradiance measurements ($E$) with global radiation (G). Fig. 4 shows that both quantities are almost linearly related. Most of the differences will be caused by more gaseous absorption (mainly water vapour) and less molecular scattering in the case of $G$. Water vapour absorption reduces $G$, not $E$. We did indeed observe smaller values of $G$ for a certain value of UV-A irradiance when clouds were present. Water vapour absorption is also enhanced in the presence of clouds due to the increase in the mean path length of photons. The good correlation between $G$ and $E$ suggests that measurements of $G$ instead of UV-A irradiances can be used to estimate photodissociation rates, although the results will be slightly less accurate.

In Fig. 5, the actinic flux as a function of $G$ is shown for clear sky conditions at different sites. The clear sky data of the Azores and De Bilt show a curvature for small zenith angles (i.e., at largest $G$ values). Fig. 5 shows the large effect that the high surface albedo (about 0.9) has on both $F$ and $G$ at the Antarctica site. In the Antarctic data some scatter is observed in the middle of the day due to a nearby mountain ridge (Bintanja et al., 1993). For these measurements the solar zenith angle is always large ($>50°$ in December). Therefore the amount of direct incident radiation is relatively small for all zenith angles. Furthermore, the diffuse downward flux is enlarged due to atmospheric backscattering. This explains the observed linear relation between $F$ and $G$.

The large difference in the slope (about 2.2) between the Antarctica data and the Azores/De Bilt data is caused mainly by the difference in $1+A$ (surface albedo) (about 1.8). Differences in atmospheric backscattering also contribute. Atmospheric backscattering is more important for

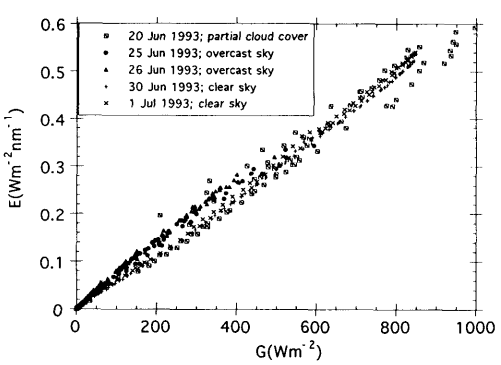


*Fig. 4.* Measured UV-A irradiance ($E$) as a function of measured global radiation ($G$) for clear sky, overcast and partial cloud cover conditions in De Bilt, the Netherlands.

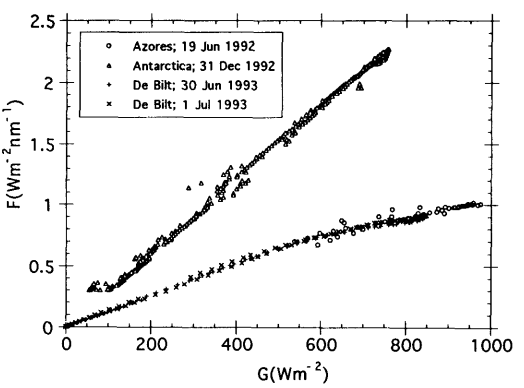


*Fig. 5.* Measured UV-A actinic flux ($F$) as a function of measured global radiation ($G$) for clear sky conditions. Measurements were performed in the Azores (19 June 1993; surface albedo 0.05), Antarctica (31 December 1992; surface albedo 0.9) and De Bilt, the Netherlands (30 June 1993 and 1 July 1993; surface albedo 0.05).

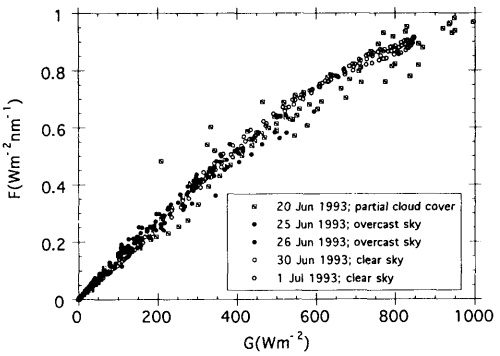


*Fig. 6.* Measured UV-A actinic flux ($F$) as a function of measured global radiation ($G$) for clear sky, overcast and partial cloud cover conditions in De Bilt, The Netherlands.

the UV-A region (i.e., for $F$) than for the total solar spectrum (G).

Fig. 6 shows UV-A actinic fluxes as a function of the simultaneously measured global radiation for clear sky, complete overcast and partial cloud cover conditions. We observe that the variation in $F$ for a given measurement of $G$ is always smaller than 20% ($A = 0.05$). Therefore, we conclude that an emperical relation between the photodissociation rate of $NO_2$ and global radiation can be accurate within 20%. Observe the curvature in the relation between UV-A actinic flux and global radiation for large values of $G$.

The expressions given by Bahe et al. (1980) and Brauers and Hofzumahaus (1992) cannot be used directly in the case of a high surface albedo, but a correction can easily be made when surface albedo is known (cf. eq. (1)). The curvature observed in Fig. 6 is not taken into account in their relationships. Therefore $J_{NO_2}$ will be underestimated for most zenith angles when linear regression is based on data that cover the whole range of solar zenith angles (Brauers and Hofzumahaus (1992)). Bahe et al. (1980) did not include values for zenith angles smaller than 30°. Therefore their empirical expression overestimates $J_{NO_2}$ for small zenith angles ($\theta_0 < 30°$) when global radiation values are largest.

Due to highly variable water vapour absorption and a smaller effect of (multiple) scattering some extra uncertainties are introduced into the estimation of photodissociation rates from global radiation measurements instead of from UV-A irradiance measurements. On the other hand we found that on a day with partial cloudiness the variation in UV-A actinic fluxes for given global radiation measurements (20%) was somewhat smaller than the variation for given UV-A irradiance measurements (25%).

## 6. Summary

This paper shows how UV-A actinic flux, UV-A irradiance and global radiation at ground level are related. Measurements of UV-A actinic flux are compared with measurements of UV-A irradiance and global radiation. It is shown that solar zenith angle, surface albedo and the ratio of direct to total incident irradiance are the most important parameters in the relation between actinic flux and irradiance. Eqs. (1) and (3) describe the effect of different geographic (ground albedo, latitude) and atmospheric conditions (aerosols, clouds) on this relationship. Uncertainties in the relation between actinic flux and downward irradiance are caused by the anisotropy of the radiation field and by the horizontal inhomogeneity of the atmosphere. When UV-A actinic flux and global radiation are compared extra uncertainties are added due to water vapour absorption and the relatively smaller effect of scattering for $G$. The effect of horizontal inhomogeneity was also illustrated with measurements of actinic flux at ground level on a day with partial cloudiness. We observed actinic fluxes that were up to 10% higher than in clear sky conditions. Combining the variation in the measured ratios of the downward irradiance and the actinic flux and the uncertainties that were estimated with model calculations we estimate that photodissociation rates can be derived from UV-A irradiance measurements within an accuracy of 10% under clear sky conditions and under completely overcast conditions (no direct radiation below the cloud). However, we found a variation of up to 25% in the measured UV-A actinic flux for given UV-A irradiance under all atmospheric conditions.

In Section 5 it was shown that UV-A actinic fluxes are related to global radiation. Further, global radiation correlates strongly with the UV-A irradiance. This supports the idea that photodissociation rates can be related to global radiation. We concluded that the expressions for the photodissociation rate of $NO_2$ as a function of



Tellus B/47/3-7

global radiation given by Bahe et al. (1980) and Brauers and Hofzumahaus (1992) does not hold for large surface albedo. However, a correction can be made for the surface albedo effect. Due to the assumed linear relation between global radiation and $J_{NO_2}$ the photodissociation rate is either underestimated or overestimated. Variations in UV-A actinic flux for a given measurement of $G$ are smaller than 20% for clear sky, overcast and partial cloud covered days. Therefore we estimate that photodissociation rates can be obtained from global radiation measurements within an accuracy of 20%.

We conclude that photodissociation rates can be measured more accurately with chemical actinometers, i.e., in the range of 5% according to (Shetter et al., 1992; Madronich, 1987), than with UV-A irradiance or global radiation measurements. However, it is often preferable to use (standard) radiometric measurements because these are less complicated and more widespread. Therefore we support that empirical relationships are established in a form equivalent to eq. (1) by simultaneous measurements of photodissociation rates with chemical actinometers, UV-A downward irradiance (direct and total) and global radiation measurements.

## 7. Acknowledgements

Some of the experimental campaigns were financially supported by the Netherlands Organization for Scientific Research (NWO) and the Dutch National Research Programme on Air Pollution and Climate Change (NRP). R. Bintanja, M. Portanger and M. van de Broeke (IMAU) made possible the measurements in Antarctica. We thank P. Stammes (KNMI) for providing his doubling-adding code for flux calculations, and, together with P. G. Duynkerke (IMAU), for making useful comments and contributions to discussions.

## 8. Appendix

The actinic flux $F$ is defined as the radiance $I$ integrated over all solid angles ($d\Omega = 2\pi\, d\mu$). The actinic flux can be split into three components, namely a direct downward flux $F_0$, a diffuse downward flux $F_\downarrow$ and a diffuse upward flux $F_\uparrow$:

$$F = F_0 + F_\downarrow + F_\uparrow \tag{A1}$$

The diffuse fluxes are defined as

$$F_\downarrow = 2\pi \int_{-1}^{0} I \, d\mu, \qquad F_\uparrow = 2\pi \int_{0}^{1} I \, d\mu, \tag{A2a, b}$$

where $\mu$ is the cosine of zenith angle.

The diffuse downward irradiance $E_\downarrow$ and the diffuse upward irradiance $E_\uparrow$ are defined as the radiance weighted with the cosine of the angle of incidence integrated over the overlying and underlying hemisphere, respectively

$$E_\downarrow = 2\pi \int_{-1}^{0} -\mu I \, d\mu, \qquad E_\uparrow = 2\pi \int_{0}^{1} \mu I \, d\mu. \tag{A3a, b}$$

The downward irradiance is the sum of $E_\downarrow$ and a direct downward flux $E_0$, where $E_0 = \mu_0 F_0$:

$$E = E_0 + E_\downarrow. \tag{A4}$$

Finally we can define an albedo $A$ as

$$A = \frac{E_\uparrow}{E}. \tag{A5}$$

Combining eqs. (A1) and (A4), one finds (with $E_0 = \mu_0 F_0$) for the exact ratio of $F$ over $E$:

$$\frac{F}{E} = \frac{F_\downarrow + F_\uparrow}{E_\downarrow} + \left( \frac{1}{\mu_0} - \frac{F_\downarrow + F_\uparrow}{E_\downarrow} \right) \frac{E_0}{E}. \tag{A6}$$

Eq. (A6) expresses the relation between the actinic flux and the downward irradiance in terms of ratios of diffuse fluxes, $\mu_0$ and the ratio of the direct to total downward irradiance $E_0/E$.

The ratios of diffuse fluxes can be calculated for a given angular distribution of the radiance. For a isotropic radiation field ($I$ is angular independent) we find

$$\frac{F_\downarrow}{E_\downarrow} = 2, \qquad \frac{F_\uparrow}{E_\uparrow} = 2. \tag{A7a, b}$$

In the Eddington approximation $I = I_0 + \mu I_1$, where $I_0$ and $I_1$ are independent of direction, we find

$$F_\downarrow + F_\uparrow = 2(E_\downarrow + E_\uparrow). \quad \text{(A8)}$$

Substituting (A7) or (A8) in (A1) both yield

$$\frac{F}{E} = 2(1 + A) + \left(\frac{1}{\mu_0} - 2\right)\frac{E_0}{E}. \quad \text{(A9)}$$

Therefore, we conclude that the ratio of actinic flux to downward irradiance in the Eddington approximation is equal to the ratio for an isotropic radiation field.

If we assume that the surface is Lambertian with albedo $A$, i.e., the upward radiation is isotropically distributed, the general relation in a horizontally homogeneous atmosphere between the actinic flux and downward irradiance just above this surface is given by

$$\frac{F}{E} = \frac{F_\downarrow}{E_\downarrow} + 2A + \left(\frac{1}{\mu_0} - \frac{F_\downarrow}{E_\downarrow}\right)\frac{E_0}{E}. \quad \text{(A10)}$$

The ratio of $F_\downarrow/E_\downarrow$ depends on wavelength, solar zenith angle and atmospheric composition. Typical ranges for this ratio in the UV-A spectral region are given in the text. Eq. (A10) is exact only for a horizontally homogeneous atmosphere and above a Lambertian surface. Higher in the atmosphere the upward radiation is generally not isotropic, and only eq. (A6) is valid.

## REFERENCES


ASTEX 1992. *ASTEX Operations Plan.* Available from the FIRE Project Office, MS 483, NASA Langley Research Center, Hampton, VA, USA.

Bahe, F. C., Schurath, U. and Becker, K. H. 1980. The frequency of $NO_2$ photolysis at ground level, as recorded by a continuous actinometer. *Atmos. Environ.* **14**, 711–718.

Bintanja, R., Van den Broeke, M. R. and Portanger, M. P. 1993. *A meteorological and glaciological experiment on a blue ice area in the Heimefront Range, Queen Maud Land, Antarctica.* SVEA 1992/1993 Field Report, Institute for Marine and Atmospheric Research Utrecht, Utrecht University, Utrecht, The Netherlands.

Brauers, T. and Hofzumahaus, A. 1992. Latitudinal variation of measured $NO_2$ photolysis frequencies over the Atlantic ocean between 50° N and 30° S. *J. Atmos. Chem.* **15**, 269–282.

Davis, D. D., Chen, G., Chameides, W., Bradshaw, J., Sandholm, S., Rodgers, M., Schendal, J., Madronich, S., Sachse, G., Gregory, G., Anderson, B., Barrick, J., Shipham, M., Collins, J., Wade, L. and Blake, D. 1993. A photostationary state analysis of the $NO_2$-NO system based on airborne observations from the subtropical/tropical North and South Atlantic. *J. Geophys. Res.* **98**, 23501–23523.

De Haan, J. F., Bosma, P. B. and Hovenier, J. W. 1987. The adding method for multiple scattering computations of polarized light. *Astronom. Astrophys.* **183**, 371–391.

Harvey, R. B., Stedman, D. H. and Chameides, W. 1977. Determination of the absolute rate of solar photolysis of $NO_2$. *J. Air Pollut. Control Ass.* **27**, 663–666.

Junkermann, W., Platt, U. and Volz-Thomas, A. 1989. A photoelectric detector for the measurement of photolysis frequencies of ozone and other atmospheric molecules. *J. Atmos. Chem.* **8**, 203–227.

King, M. and Harsvardhan, 1986. Comparative accuracy of selected multiple scattering approximations. *J. Atmos. Sci.* **43**, 784–801.

Liou, K. N. 1992. *Radiation and cloud processes in the atmosphere.* Oxford Univ. Press, New York.

Madronich, S. 1987a. Intercomparison of $NO_2$ photodissociation and u.v. radiometer measurements. *Atmos. Environ.* **21**, 569–578.

Madronich, S. 1987b. Photodissociation in the atmosphere, 1, Actinic flux and the effect of ground reflections and clouds. *J. Geophys. Res.* **92**, 9740–9752.

Nader, J. S. and White, N. 1969. Volumetric measurements of ultraviolet energy in an urban atmosphere. *Envir. Sci. Technol.* **3**, 848–854.

Ruggaber, A., Forkel, R. and Dlugi, R. 1993. Spectral actinic flux and its ratio to irradiance by radiation transfer calculations. *J. Geophys. Res.* **98**, 1151–1162.

Shetter, R. E., McDaniel, A. H., Cantrell, C. A., Madronich, S. and Calvert, J. G. 1992. Actinometer and Eppley radiometer measurements of the $NO_2$ photolysis rate coefficient during the Mauna Loa Observatory Photochemistry EXperiment. *J. Geophys. Res.* **97**, 10349–10359.

Shettle, E. P. and Weinman, J. A. 1970. The transfer of solar irradiance through inhomogeneous atmospheres evaluated by Eddington's approximation. *J. Atmos. Sci.* **27**, 1048–1055.

Stammes, P. 1993. Influence of clouds on shortwave flux profiles and polarization. In: *IRS '92: Current problems in atmospheric radiation*, (eds. S. Keevallik and O. Kärner). A. Deepak Publ., Hampton, VA, USA.

Stammes, P., De Haan, J. F. and Hovenier, J. W. 1989. The polarized internal radiation field of a planetary atmosphere. *Astronom. Astrophys.* **225**, 239–259.

Toon, O. B., McKay, C. P., Ackerman, T. P. and Santhanam, K. 1989. Rapid calculations of radiative heating rates and photodissociation rates in inhomogeneous multiple scattering atmospheres. *J. Geophys. Res.* **94**, 16287–16301.

Van de Hulst, H. C. 1980. *Multiple light scattering*, vols. 1, 2, Academic Press, New York.

Van der Hage, J. C. H. 1992. Actinic flux and global radiation. *Theor. Appl. Climatol.* **46**, 173–177.

Van der Hage, J. C. H., Boot, W., Van Dop, H., Duynkerke, P. G. and Vilà-Guerau de Arellano, J. 1994. A photo-electric detector suspended under a balloon for actinic flux measurements. *J. Atmos. Ocean Technol.* **11**, 674–679.

Van Weele, M. and Duynkerke, P. G. 1993. Effect of clouds on the photodissociation of $NO_2$: observations and modelling. *J. Atmos. Chem.* **16**, 231–255.

Vilà-Guerau de Arellano, J., Duynkerke, P. G. and Van Weele, M. 1994. Tethered-balloon measurements of actinic flux in a cloud-capped marine boundary layer. *J. Geophys. Res.* **99**, 3699–3705.

Warren, S. G., Brandt, R. E. and Boime, R. D. 1993. Blue ice and green ice. *Antarctic J. of the United States* **28**, 255–256.

Zafonte, L., Rieger, P. L. and Holmes, J. R. 1977. Nitrogen dioxide photolysis in the Los Angeles atmosphere. *Envir. Sci. Technol.* **11**, 483–487.